Uzbek Journal of Physics
DOI: https//doi.org/10.52304/.v25i4.471

Investigation of intermolecular interactions in butyl acetate using vibrational spectroscopy and non-empirical calculations

A. Jumabaev*, A.A. Absanov, B.B. Khudaykulov, Z.I. Ernazarov

Samarkand State University, University blv. 15, 140104, Samarkand, Uzbekistan

Received 25.08.2023, revised 26.12.2023

* Corresponding author: e-mail jumabaev2@rambler.ru, Phone: +998 93 728 77 01

В данной работе на примере бутилацетата исследована природа сил межмолекулярного взаимодействия с использованием колебательной спектроскопии (КР и FTIR) и неэмпирических расчетов. Геометрические структуры наиболее стабильных димерных и тримерных агрегатов бутилацетата оптимизированы с использованием метода теории функционала плотности (DFT) на основе базиса B3LYP/6-311++G(d,p). Показано, что молекулярные агрегаты в жидком бутилацетате образуются за счет диполь-дипольных взаимодействий и слабых водородных связей C-H…O. Для молекулы бутилацетата был проведен анализ распределения потенциальной энергии (PED) и обнаружено, что экспериментальные и расчетные частоты хорошо согласуются. Проанализированы граничные молекулярные орбитали, такие как высшая занятая молекулярная орбиталь (HOMO) и низшая незанятая молекулярная орбиталь (LUMO) молекулы бутилацетата.

Ключевые слова: бутилацетат, комбинационное рассеяние света, FTIR, водородная связь, DFT, PED-анализ.

In this work, on the example of butyl acetate, the nature of intermolecular interactions was studied using vibrational spectroscopy (Raman and FTIR) and non-empirical calculations. The geometric structures of the most stable dimer and trimer aggregates of butyl acetate were optimized using the Density Functional Theory (DFT) method based on the B3LYP/6-311++G(d,p) basis set. Molecular aggregations in liquid butyl acetate were shown to be formed by dipole-dipole interactions and weak C-H…O hydrogen bonds. A potential energy distribution (PED) analysis was performed for the butyl acetate molecule, and experimental and calculated frequencies were found to be in good agreement. Frontier molecular orbitals such as the highest occupied molecular orbital (HOMO) and lowest unoccupied molecular orbital (LUMO) of the butyl acetate molecule were analyzed.

Keywords: butyl acetate, Raman spectroscopy, FTIR, hydrogen bonding, DFT, PED analysis.

I. Introduction

Intermolecular interactions play a key role in the study of physical, biological, and chemical processes [1, 2]. Vibrational spectroscopy and theoretical calculations are widely used to study the nature of intermolecular interaction forces [3-7]. Researchers have been interested in the study of intermolecular interactions in ethers and their solutions for many years [8-12]. The butyl acetate molecule belonging to the group of ethers has the chemical structure $C_6H_{12}O_2$, and the dipole moment is equal to 1.87 D. Butyl acetate is a colorless transparent liquid that is mainly used as a solvent in the production of paints and varnishes [13-15].

It was found in solutions of methyl sulfonic acid in butyl acetate that molecular and ionic complexes are in equilibrium: when dissolved in the neutral solvent tetrachloroethane, IR spectra indicate an increase in the concentration of undissociated acid molecules and a decrease in the concentration of proton solvates [16]. The hydrogen bonding interaction between butyl acetate and 2-alkyl ethanols was confirmed by

FTIR spectra. The maximum frequency of the C=O vibration band of pure butyl acetate corresponds to 1762 cm^{-1}, and this frequency in mixtures of butyl acetate with 2-butoxyethanol, 2-ethoxyethanol, and 2-methyloxyethanol is observed at 1743, 1742, and 1740 cm^{-1}, respectively. It has been shown that these changes can be caused by weak interactions such as dispersion, dipole-dipole, or H-bonding in liquid mixtures [17].

Studying the interaction between butyl acetate and p-nitrophenol molecules shows, one molecule of butyl acetate interacts with p-nitrophenol through hydrogen bonding, and the second butyl acetate molecule interacts with p-nitrophenol through dipole-dipole interaction. It was also found that the number of butyl acetate molecules in the outer sphere can depend on the concentration of free butyl acetate molecules in the solutions. In this case, the C=O vibration band of butyl acetate involved in hydrogen bonding was observed at 1707 cm^{-1} [18].

From the review of the above literature, it can be seen that intermolecular interactions in liquid butyl acetate have not been fully studied. In this work, the spectral manifestation of intermolecular interactions in pure butyl acetate was studied using Raman and FTIR spectroscopies. The formation mechanism of molecular aggregations was analyzed by the DFT method. Potential energy distribution (PED) analysis was carried out in order to determine the percentage of vibrational energies in the molecule. Also, the reactivity of the butyl acetate molecule was evaluated using frontier molecular orbital (FMO) analysis.

II. Experimental and theoretical methods

Raman spectra were obtained on a diffraction-grating InViaRaman spectrometer with a period of 1200 lines/mm. The exposure time is 10 s, and the resolution is 0.01 cm^{-1}. A spectrum stabilised laser module with a wavelength of 532 nm and a power of 50 mW was used as a source of excitation light. The scattered light was recorded using a Renishaw CCD camera detector. FTIR spectra were obtained on an IRAffinity-1S Fourier spectrometer and analysed using LabSolutions IR software. Redistilled and chemically purified butyl acetate was used in the experiments. All experiments were conducted at room temperature. All calculations were performed in the Gaussian 09 program [19] using the B3LYP/6-311+G(d,p) DFT method. PED analysis was performed using VEDA 4.0 software [20].

III. Results and discussion

III.1. Vibrational frequency analysis

Figure 1 shows experimental Raman and FTIR spectra of liquid butyl acetate.

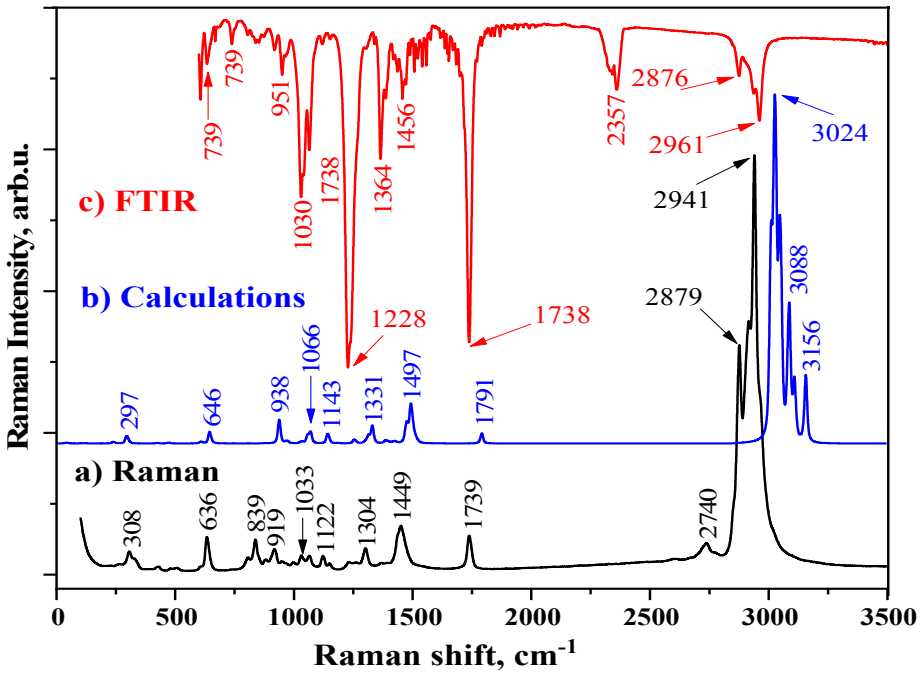


Figure 1. Experimental Raman and FTIR spectra of liquid butyl acetate.

©Академия наук Республики Узбекистан, 2023 г.

These spectral bands are complex and have several vibrational maxima. The bands observed in Raman and FTIR coincide with each other. Since the intensities of Raman spectra depend on the dipole moment, and the intensities of FTIR spectra depend on polarizability, some bands are active in Raman scattering, while others are active in FTIR. When we focus on C=O and C-H vibrational bands involved in intermolecular interactions, the C=O vibrational band is observed at 1739 cm^{-1} in Raman and 1738 cm^{-1} in FTIR and has higher intensity compared to Raman. The C-H band in the methyl group of butyl acetate was observed at 2879 and 2941 cm^{-1} in Raman and 2876 and 2961 cm^{-1} in FTIR, and the intensity of the C-H vibrational band was observed to be higher in Raman than in FTIR. The intensity of the remaining frequencies is very low.

A PED analysis was performed for the butyl acetate molecule and the calculated and experimental frequencies were compared (Table 1). Through this analysis, the percentages (%) of the vibrational potential energies of the atomic group of vibrations in the molecule were determined. It can be seen from the table, that the difference between the experimental and theoretical calculations is greater in the values of the four vibration frequencies. These are *v* stretching (CH) ((difference 5% (4% in FTIR), experiment 2941 cm^{-1} (2961 cm^{-1} in FTIR) and calculation 3082 cm^{-1})), *n* stretching (CH) (difference 5%, experiment 2879 cm^{-1} (2876 cm^{-1} in FTIR and 3024 cm^{-1} in calculation), with the largest difference *n* stretching (CH) (difference 9%, experiment 2740 cm^{-1} and calculation 3009 cm^{-1}), *n* stretching (CC) and the vibrational frequency of the system consisting of a combination of τ torsional ring (HCCC) (5% difference, 839 cm^{-1} in experiment and 881 cm^{-1} in calculation). The difference in the remaining frequencies is ±4% (Fig. 1).

III.2. Optimal geometries of butyl acetate aggregates

Non-empirical calculations show, there are different aggregates in liquid butyl acetate, and Fig. 2 shows monomer (a), dimer (b), and trimer (c) aggregates of butyl acetate. The dipole moment of the butyl acetate monomer is 2.16 D. At dimer formation, the O2 atom of the C=O group of the first molecule and the H40 atom of the C-H group of the neighboring molecule form a non-classical hydrogen bond in the form of C-H…O with a length of 2.436 Å, and the C-H of the first molecule. The H20 atom of the group forms a cyclic structural aggregate with the O22 atom of the C=O group of the neighboring molecule through a non-classical hydrogen bond in the form of C-H…O with a bond length of 2.436 Å. This H-bond energy is 2.58 kcal/mol.

In Figure 2c, for the trimer case of the butyl acetate molecule, the O2 atom of the C=O group of the first molecule forms a non-classical weak hydrogen bond of the form C-H…O with a length of 2.362 Å with the H40 atom of the C-H group of the second molecule. The O22 atom of the C=O group of the second molecule forms a non-classical hydrogen bond of the form C-H…O with a length of 2.375 Å with the H60 atom of the C-H group of the third molecule. The O42 atom of the C=O group of the third molecule forms a weak hydrogen bond of 2.362 Å with the H19 atom of the C-H group of the first molecule, which together forms a closed structure trimer with an energy of 5.02 kcal/mol. According to calculations, the formation of a trimer forms complexes with a closed structure through three H-bonds.

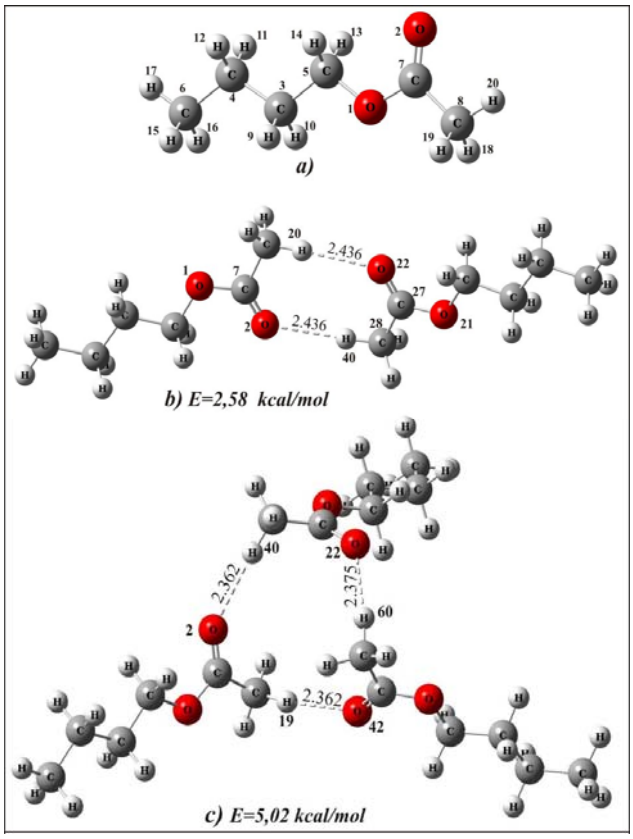


Figure 2. Optimal geometric structures of monomer (a), dimer (b), and trimer (c) of butyl acetate.

©Академия наук Республики Узбекистан, 2023 г.

Table 1. Vibrational frequencies and assignments of normal modes of butyl acetate.

Mode No.	Observed		Calcu-lated	Observed/Calculated		Assignment PED (%)
(i)	Raman	IR		Raman	IR	
1			3156			−17% ν(CH), 83% ν(CH)
2			3109			−100% ν(CH)
3			3092			−16% ν(CH), 76% ν(CH)
4			3088			88% ν(CH)
5	2941	2961	3082	0.95	0.96	−83% ν(CH)
6			3057			−82% ν(CH), 11% ν(CH)
7			3050			99% ν(CH)
8			3045			94% ν(CH)
9			3031			95% ν(CH)
10	2879	2876	3024	0.95	0.95	83% ν(CH)
11			3020			−89% ν(CH)
12	2740		3009	0.91		91% ν(CH)
13	1739	1738	1791	0.97	0.97	88% ν(OC)
14			1521			75% β(HCH), −13% τ(HCCO)
15			1509			74% β(HCH)
16			1500			−76% β(HCH), 12% τ(HCCO)
17			1497			66% β(HCH), −10% τ(HCCC)
18			1492			83% β(HCH)
19			1477			−75% β(HCH), 24% τ(HCCO)
20	1449	1456	1472	0.98	0.99	−37% β(HCH), 42% β(HCH), −19% τ(HCCO)
21			1425			12% β(HCH), −55% τ(HCCO)
22			1414			89% β(HCH)
23			1397			72% β(HCH)
24		1364	1385		0.98	10% β(HCH), −62% τ(HCCO)
25	1304		1331	0.98		76% β(HCH)
26			1314			−64% β(HCC)
27			1300			−72% τ(HCCO)
28			1258			−50% ν(CC), 15% τ(HCCO)
29	1233	1228	1253	0.98	0.98	46% β(HCC), −10% τ(HCCO), 18% τ(HCCO)
30			1186			31% β(HCC), −44% τ(HCCO)
31			1143			−17% ν(CC), 11% β(CCO), −15% β(CCC), 23% τ(HCCC)
32			1070			−76% ν(CC)
33			1066			−21% β(HCH), 57% τ(HCCO), 21% τ(OCOC)
34	1033	1030	1059	0,97	0,97	−16% ν(CC), 36% ν(OC), -22% τ(HCCO)
35			1033			−57% ν(CC), 12% τ(HCCO)
36		951	970			−11% ν(CC), 15% ν(CC), −31% ν(OC), −18% τ(HCCO)
37	919		954	0.96		−12% β(HCC), 58% τ(HCCO)
38			938			36% ν(CC), 10% β(CCO), −18% τ(HCCC)
39	839		881	0.95		−54% ν(CC), −11% τ(HCCC)
40			811			77% τ(HCCC)
41		739	747			−77% τ(HCCO)
42	636	633	646	0.98	0.97	−21% ν(CC), 10% ν(CC), 50% β(CCC)
43			608			16% τ(HCCO), −71% τ(OCOC)
44			472			−10% ν(CC), 73% β(CCC)
45			425			−68% β(CCC), 10% β(CCC)
46	308		297	104		16% ν(CC), 14% ν(OC), −48% β(CCO)
47			244			87% τ(HCCC)
48			240			−79% β(CCC)

©Академия наук Республики Узбекистан, 2023 г.

Продолжение таблицы 1.

49	188	76% τ(CCCO)
50	121	−11% τ(HCCO), 75% τ(CCCC)
51	100	89% β(CCC)
52	78	77% τ(CCCO)
53	45	−13% τ(HCCO), 64% τ(CCOC)
54	38	73% τ(HCCO), 14% τ(CCOC)

Abbreviations: ν, stretching; β, bending; τ, torsional; “minus”-asymmetric

Table 2. Charge distribution and bond length in butyl acetate aggregates.

Atoms	Atomic charge (arb.u.)			Atoms	Bond length (Å)		
	Monomer	Dimer	Trimer		Monomer	Dimer	Trimer
O^1	−0.045844	−0.017862	0.028779	C^8-H^{18}	1.09242	1.09130	1.08959
O^2	−0.280528	−0.284794	−0.283932	C^8-H^{19}	1.09244	1.09421	1.09498
C^3	−0.219889	−0.187842	−0.165415	C^8-H^{20}	1.08788	1.08893	1.08987
C^4	−0.094540	-−0.119138	−0.114963	C^8-C^7	1.50805	1.50523	1.50331
C^5	−0.328258	−0.287468	−0.345263	C^7=O^2	1.20707	1.21024	1.21141
C^6	−0.582219	−0.591637	−0.596001	C^7-O^1	1.35110	1.35116	1.34954
C^7	0.255216	0.224248	0.043808	O^1-C^5	1.44861	1.44763	1.44758
C^8	−0.563982	−0.652542	−0.521763	C^5-H^{13}	1.09325	1.09329	1.09323
H^9	0.145131	0.146081	0.141926	C^5-H^{14}	1.09324	1.09333	1.09337
H^{10}	0.145196	0.144476	0.146653	C^5-C^3	1.51852	1.51873	1.51870
H^{11}	0.123249	0.123335	0.123034	C^3-H^9	1.09557	1.09558	1.09551
H^{12}	0.123195	0.122725	0.125370	C^3-H^{10}	1.09557	1.09553	1.09557
H^{13}	0.197192	0.194670	0.196111	C^3-C^4	1.53373	1.53375	1.53363
H^{14}	0.197194	0.196588	0.180080	C^4-H^{11}	1.09649	1.09653	1.09658
H^{15}	0.134528	0.135112	0.134979	C^4-H^{12}	1.09649	1.09650	1.09654
H^{16}	0.134495	0.134821	0.135879	C^4-C^6	1.53132	1.53137	1.53137
H^{17}	0.142851	0.141508	0.140906	C^6-H^{15}	1.09433	1.09434	1.09433
H^{18}	0.170970	0.158858	0.148943	C^6-H^{16}	1.09434	1.09434	1.09433
H^{19}	0.171039	0.169434	0.334949	C^6-H^{17}	1.09316	1.09323	1.09324
H^{20}	0.175005	0.249436	0.145145				

Table 2 presents the charge distribution and geometric parameters for the monomer, dimer, and trimer of butyl acetate and its derivatives. It can see in the table that the charge distributions and the lengths of the chemical divisions of the atoms involved in hydrogen splitting have changed. Atoms O1, O2, C3, C4, C5, C6, and C8 in the molecule are negatively charged, while the remaining atoms are positively charged.

Figure 3 shows the Raman spectra of the calculated C=O vibration of butyl acetate, which corresponds to 1791 cm^{-1} in the monomer state. In the case of the dimer, this spectral line corresponds to 1772 cm^{-1} and shifts to a lower frequency by 19 cm^{-1} compared to the monomer. Since the Raman activity of the vibration at 1782 cm^{-1} is zero, this spectral line doesn’t appear. In the trimer, these bands are splitted into three parts: 1763, 1773.8, and 1774.3 cm^{-1}, respectively. The 1773.8 cm^{-1} and 1774.3 cm^{-1} lines

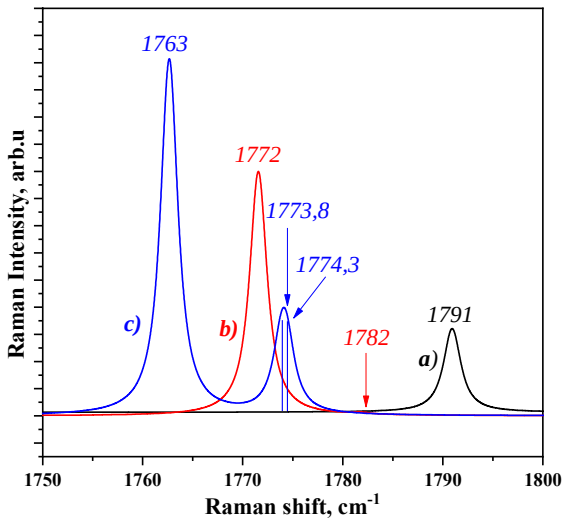


Figure 3. Calculated Raman spectra of C=O stretching vibration of butyl acetate: monomer (a), dimer (b), trimer (c).

©Академия наук Республики Узбекистан, 2023 г.

are close to each other, and for this reason they are one band in the O2 atom in the C=O group of the first molecule of butyl acetate. In this case, butyl acetate is bonded by the O2 atom in the C=O group of the first molecule and the H40 atom in the CH3 group of the second molecule. It bonded with the O42 atom of the C=O group of the third molecule and the H19 atom of the CH3 group of the first molecule. This bond is a weak hydrogen bond with bond length is 2.362 Å. It can be seen from the figure that the C=O vibrational band in the case of the trimer is more shifted to the low-frequency side compared to the monomer (shifted to 28 cm^{-1}).

III.3. Frontier molecular orbital (FMO) analysis

With the help of theoretical calculations, it is possible to obtain information about the orbitals of a molecule and the transitions between them. The highest occupied molecular orbital (HOMO) and the lowest unoccupied molecular orbital (LUMO) are also called frontier molecular orbitals. The energy difference between HOMO and LUMO is the energy gap, and it plays an important role in chemical stability. Also, this energy gap (HOMO-LUMO) is used to display the intramolecular charge transfer, kinetic polarisation, and electronic spectra of a molecule or molecular system [21-23]. Quantum chemical parameters such as global electrophilicity index, hardness, softness, electron affinity, and ionization energy can calculate using the Koopmans theorem [24]. Frontier molecular orbitals of butyl acetate are shown in Fig. 4. Using the HOMO and LUMO energies, various quantum chemical parameters (Table 3) such as ionization energy (*IE*), chemical potential (μ), hardness (ε), electron affinity (*EA*), and global electrophilicity index (ω) were calculated using the following relations:

hardness $\eta=(E_{HOMO}-E_{LUMO})/2$; chemical potential $\mu=(E_{HOMO}+E_{LUMO})/2$; global electrophilic index $\omega=\mu^2/2\eta$; ionization energy $IE= -E_{HOMO}$; electron affinity $EA = -E_{LUMO}$.

Table 3. Some quantum-chemical parameters of butyl acetate.

E_{HOMO}	–0.282 eV
E_{LUMO}	–0.011 eV
$E_{HOMO}-E_{LUMO}$	0.271 eV
Hardness	0.136 eV
Chemical potential	–0.147 eV
Global electrophilic index	0.079
$IE=-E_{HOMO}$	0.282 eV
$EA= - E_{LUMO}$	0.011 eV

Molecules with a large HOMO-LUMO energy difference are stable and less reactive, while molecules with a low HOMO-LUMO energy difference are reactive. The HOMO-LUMO energy difference of butyl acetate is 0.27 eV, which indicates that it is a reactive molecule (Table 3).

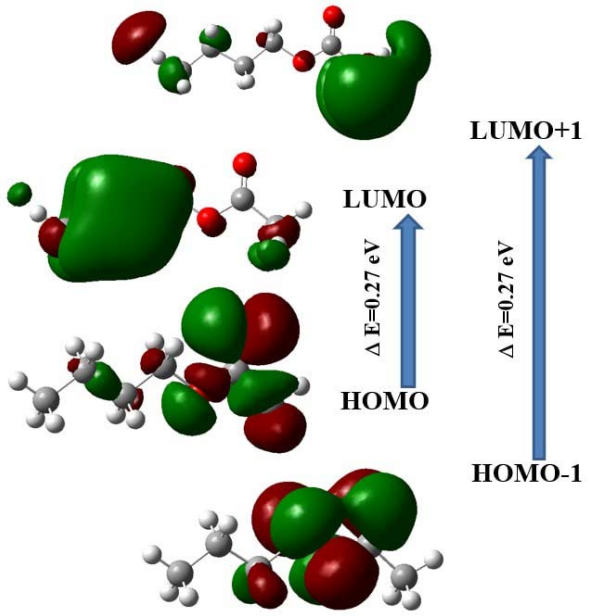


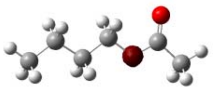
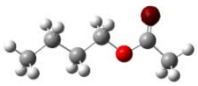
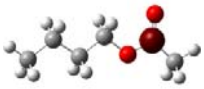
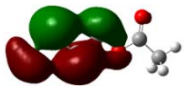
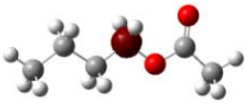
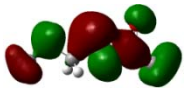
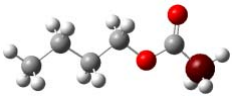
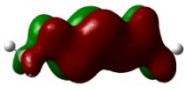
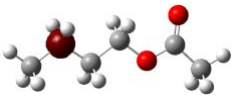
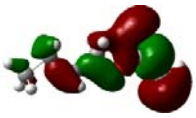
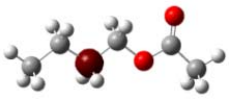
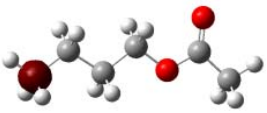
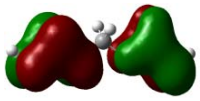
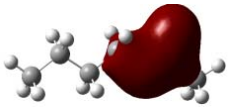
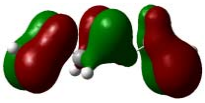
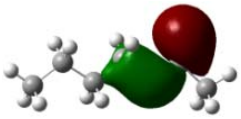
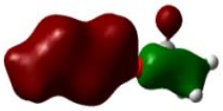
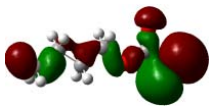
Figure 4. Frontier molecular orbital diagram of butyl acetate.

Table 4 lists the HOMO and LUMO and other orbital energies and the shape of the orbital. The electron molecular orbital becomes full in the HOMO orbital, and the next unfilled orbital becomes LUMO. It also determines the threshold of transition of the electron to the excited state and the energy in the orbitals.

The total number of electrons in butyl acetate is 64, and these electrons with opposite spin occupy 32 orbitals. The last 32-nd HOMO has energy of –0.282 eV and LUMO energy is of –0.011 eV, and the difference between them is –0.271 eV, which represents the energy required for an electron to move from the highest filled orbital to the next unfilled orbital. It can be seen from the table 4 that the lowest orbital of butyl acetate corresponds to HOMO-31, and the energy corresponding to this state is -19.168 eV and differs from the HOMO energy by 18.886 eV.

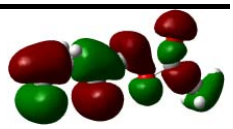
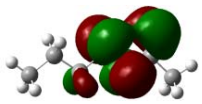
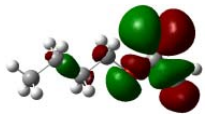
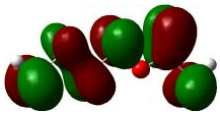
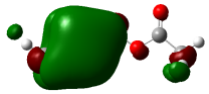
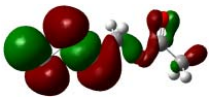
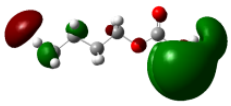
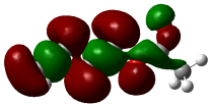
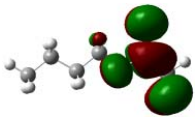
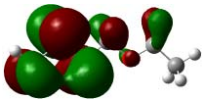
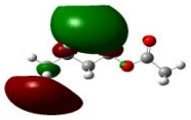
©Академия наук Республики Узбекистан, 2023 г.

Table 4. Energies and shapes of the molecular orbitals of butyl acetate.

No.	Name of orbital	Energy (ev)	Shape of orbital	No.	Name of orbital	Energy (ev)	Shape of orbital
1	HOMO-31	–19.168		13	HOMO-19	–0.729	
2	HOMO-30	–19.113		14	HOMO-18	–0.652	
3	HOMO-29	–10.306		15	HOMO-17	–0.595	
4	HOMO-28	–10.229		16	HOMO-16	–0.571	
5	HOMO-27	–10.183		17	HOMO-15	–0.507	
6	HOMO-26	–10.177		18	HOMO-14	–0.497	
7	HOMO-25	–10.176		19	HOMO-13	–0.478	
8	HOMO-24	–10.166		20	HOMO-12	–0.470	
9	HOMO-23	–1.109		21	HOMO-11	–0.437	
10	HOMO-22	–1.023		22	HOMO-10	–0.435	
11	HOMO-21	–0.814		23	HOMO-9	–0.414	

Continied Table 4

©Академия наук Республики Узбекистан, 2023 г.

12	HOMO-20	–0.769		24	HOMO-8	–0.409	
25	HOMO-7	–0.392		31	HOMO-1	–0.310	
26	HOMO-6	–0.368		32	HOMO	–0.282	
27	HOMO-5	–0.365		33	LUMO	–0.011	
28	HOMO-4	–0.349		34	LUMO+1	–0.003	
29	HOMO-3	–0.347		35	LUMO+2	–0.001	
30	HOMO-2	–0.339		36	LUMO+3	0.009	

IV. Conclusions

In this work, the PED analysis for butyl acetate was conducted, and the theoretically determined frequencies were in good agreement with the experimentally obtained frequencies. These frequencies agree with the experimental values within ±4%. It was observed that the maxima of the spectral lines corresponding to C=O and C-H stretching vibrations in the experimentally recorded Raman spectra of liquid butyl acetate correspond to 1739.5 cm^{-1} (half-width 20.7 cm^{-1}) and 2941.3 cm^{-1}, respectively. During the formation of dimer and trimer complexes, it was observed that, due to intermolecular interactions, the spectral line corresponding to the C=O vibration shifts to a lower frequency by 19 and 28 cm^{-1} compared to the monomer. The total number of electrons in butyl acetate is 64, and these electrons with opposite spin occupy 32 orbitals. The difference between the last 32-orbital HOMO energy is –0.282 eV and the LUMO energy is –0.011 eV, and the difference is –0.271 eV.

Acknowledgments. This work is supported by a project number Ф3-20200929385, Ministry of Higher Education, Science and Innovation, Republic of Uzbekistan.

References

[1] I.G. Kaplan. Intermolecular Interactions: Physical Picture, Computational Methods and Model Potentials (John Wiley & Sons Ltd, 2006).

[2] A. Stone. The Theory of Intermolecular Forces, 2nd Edition (Oxford University Press, 2013).

[3] F.H. Tukhvatullin, B.G. Hudayberdiev, A. Jumabaev, H.A. Hushvaktov, A. Absanov. J. Mol. Liq. **155**, No.1, 67-70 (2010). https://doi.org/10.1016/j.molliq.2010.05.015.

[4] Yu. Zhou, Zonghua Wang, Shida Gong, Zhiwu Yu, Xianzhen Xu. J. Mol. Struct. **1173**, 321-327 (2018). https://doi.org/10.1016/j.molstruc.2018.07.012.

©Академия наук Республики Узбекистан, 2023 г.

[5] H. Hushvaktov, A. Jumabaev, I. Doroshenko, A. Absanov. Vib. Spectrosc. **117**, 103315 (2021). https: //doi.org/10.1016/j.vibspec.2021.103315.
[6] H. Hushvaktov, B. Khudaykulov, A. Jumabaev, I. Doroshenko, A. Absanov, G. Murodov. Mol. Cryst. Liq. **749**, 124–131 (2022). https://doi.org/10.1080/15421406.2022.2068478
[7] H.A. Hushvaktov, F.H. Tukhvatullin, A. Jumabaev, U.N. Tashkenbaev, A.A. Absanov, B.G. Hudoyberdiev, B. Kuyliev. J. Mol. Struc. **1131**, 25-29 (2017). https://doi.org/10.1016/j.molstruc.2016.10.061
[8] M.A. Natal-Santiago, M. Hill Josephine, J.A. Dumesic. J Mol Catal A Chem. **140**, 199-214 (1999). https://doi.org/10.1016/S1381-1169(98)00231-3
[9] G. Arivazhagan, R. Shanmugam, A. Elangovan. Spectrochimica Acta Part A: Molecular and Biomolecular Spectroscopy **81**, 172-177 (2011). https://doi.org/10.1016/j.saa.2011.05.097
[10] B.G. Oliveira, R.C.M.U. Araujo, A.B. Carvalho, M.N. Ramos. Spectrochimica Acta Part A: Molecular and Biomolecular Spectroscopy **68**, 626-631 (2007). https://doi.org/10.1016/j.saa.2006.12.038
[11] P. Sivagurunathan, K. Dharmalingam, K. Ramachandran, Spectrochimica Acta Part A: Molecular and Biomolecular Spectroscopy **64**, 127-129 (2006). https://doi.org/10.1016/j.saa.2005.07.005
[12] D. Ramachandran, K. Rambabu, P. Venkateswarlu, K. Mohankrishnan, G. K. Raman. Phys. Chem. Liq. **33,** No.1, 1-16 (1996). https://doi.org/10.1080/00319109608030542
[13] G.V Buxton, J. Wang, G.A Salmon. Phys. Chem. Chem. Phys. **3**, No.13, 2618-2621 (2001). https://doi.org/10.1039/B101932P
[14] W. Riemenschneider, B. Hermann. Ullmann's Encyclopedia of Industrial Chemistry (Weinheim, Wiley-VCH, 2005). https://doi.org/10.1002/14356007.a09_565.pub2
[15] Y. Lv, Y. Jiang, J. Lu, H. Gao, W. Dong, J. Zhou, M. Jiang. Biotechnology for Biofuels, **14**, 1-13 (2021). https://doi.org/10.1186/s13068-021-02053-2
[16] V.D. Maiorov, G.I. Voloshenko, N.B. Librovich. Russ. J. Phys. Chem. **2**, 362-365 (2008). https://doi.org/10.1134/S1990793108030056
[17] S. Kumar, L. Guganathan. J. Emerg. Technol. Innov. Res. **5**, No.11, 544-554 (2018).
[18] E.L. Smol'skaya, E.S. Stoyanov, P.L. Egutkin. Bulletin of the Academy of Sciences of the USSR. Division of Chemical Science. **40**, 514-520 (1991). https://doi.org/10.1007/BF00957986
[19] M.J. Frisch, G.W. Trucks, H.B. Schlegel, G.E. Scuseria, M.A. Robb, J.R. Cheeseman, G. Scalmani, V. Barone, B. Mennucci, G.A. Petersson, H. Nakatsuji, M. Caricato, X. Li, H.P. Hratchian, A.F. Izmaylov, J. Bloino, G. Zheng, J.L. Sonnenberg, M. Hada, M. Ehara, K. Toy-ota, R. Fukuda, J. Hasegawa, M. Ishida, T. Nakajima,Y. Honda, O. Kitao, H. Nakai, T. Vreven, J.A. Montgomery, jr., J.E. Peralta, F. Ogliaro, M. Bearpark,J.J. Heyd, E. Brothers, K.N. Kudin, V.N. Staroverov, R. Kobayashi, J. Normand, K. Raghavachari, A. Rendell, J.C. Burant, S.S. Iyengar, J. Tomasi, M. Cossi, N. Rega, J.M. Millam, M. Klene, J.E. Knox, J.B. Cross, V. Bakken, C. Adamo, J. Jaramillo, R. Gomperts, R.E. Stratmann, O. Yazyev, A.J. Austin, R. Cammi, C. Pomelli, J.W. Ochterski, R.L. Martin, K. Morokuma, V.G. Zakrzewski, G.A. Voth, P. Salvador, J.J. Dannenberg, S. Dapprich, A.D. Daniels, O. Farkas, J.B. Foresman, J.V. Ortiz, J. Cioslowski, D.J. Fox. Revision A.02. Gaussian 09 (Gaussian, Inc., Wallingford CT, 2010)
[20] M.H. Jamroz. Vibrational Energy Distribution Analysis VEDA 4 (Warsaw, 2004-2010).
[21] I. Fleming. Frontier Orbitals and Organic Chemical Reactions (Wiley, London, 1976).
[22] U. Holikulov. Uzbek Journal of Physics, **25**, No.1, 46-54 (2023). https://doi.org/10.52304/.v25i1.405
[23] A. Jumabaev, U. Holikulov, H. Hushvaktov. N. Issaoui, A. Absanov. J. Mol. Liq. **377**, 121552 (2023). https://doi.org/10.1016/j.molliq.2023.121552
[24] T. Koopmans. Über die Zuordnung von Wellenfunktionen und Eigenwerten zu den Einzelnen Elektronen Eines Atoms, Physica **1**, 104-113 (1934). https://doi.org/10.1016/S0031-8914(34)90011- 2

Бутил асетатдаги молекулалараро таъсирларни тебраниш спектроскопияси ва ноэмпирик ҳисоблашлар ёрдамида ўрганиш

А. Жумабаев, А.А. Абсанов, Б.Б. Худайқулов, З.И. Эрназаров

Самарқанд давлат университети, Университет хиёбони 15, 140104, Самарқанд, Ўзбекистон

Ушбу ишда бутил асетат мисолида молекулалараро ўзаро таъсирлар табиати тебраниш спектроскопияси (Раман ва FTIR) ва ноэмпирик ҳисоблашлар ёрдамида ўрганилди. Бутил асетатнинг энг барқарор димер ва тример агрегатларининг геометрик структуралари B3LYP/6-311++G(d,p) базислари тўплами асосида зичлик функционал назарияси (DFT) усули ёрдамида оптималлаштирилди. Суюқ бутил асетатдаги молекуляр агрегатлар дипол-дипол ўзаро таъсирлари ва кучсиз C-H...O водород боғланишлари натижасида ҳосил бўлиши кўрсатилган. Бутил асетат молекуласи учун потенциал энергия тақсимоти (PED) таҳлили ўтказилди ва экспериментал ҳамда ҳисобланган частоталар ўзаро мос келиши аниқланди. Бутил асетат молекуласининг энг юқори эгалланган молекуляр орбитали (HOMO) ва энг паст банд бўлмаган молекуляр орбитали (LUMO) каби чегаравий молекуляр орбиталлари таҳлил қилинди.

Калит сўзлар: бутил асетат, Раман, FTIR, водород боғланиш, DFT, PED таҳлил.

©Академия наук Республики Узбекистан, 2023 г.